Supporting Information with Micro-electrophoresis of silica rods using confocal microscopy

Henriëtte E. Bakker,* Thijs H. Besseling, Judith E. G. J. Wijnhoven, Peter H. Helfferich, Alfons van Blaaderen,* and Arnout Imhof*

Department of Physics, Utrecht University, Utrecht

E-mail: h.e.bakker1@uu.nl; a.vanblaaderen@uu.nl; a.imhof@uu.nl

*To whom correspondence should be addressed

Supporting Figures

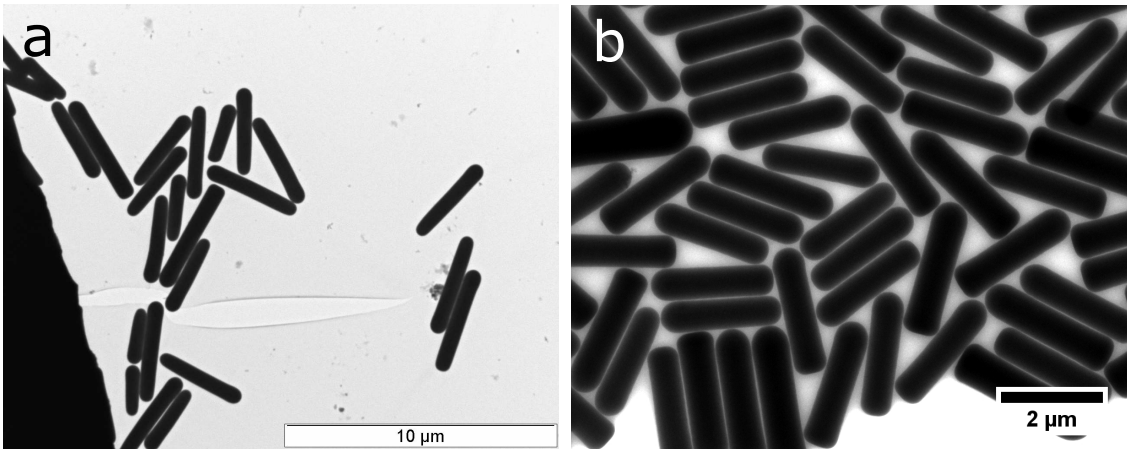

Figure S1: TEM images of particles used. (a) R2 rods, with $L = 3.6\ \mu m$ ($\delta_L \simeq 18\%$), $D = 0.59\ \mu m$ ($\delta_D \simeq 10\%$), $L/D = 6.1$ (b) SR29 rods, with $L = 2.3\ \mu m$($\delta_L \simeq 6\%$), $D = 0.60\ \mu m$ ($\delta_D \simeq 6.5\%$), $L/D = 3.8$.

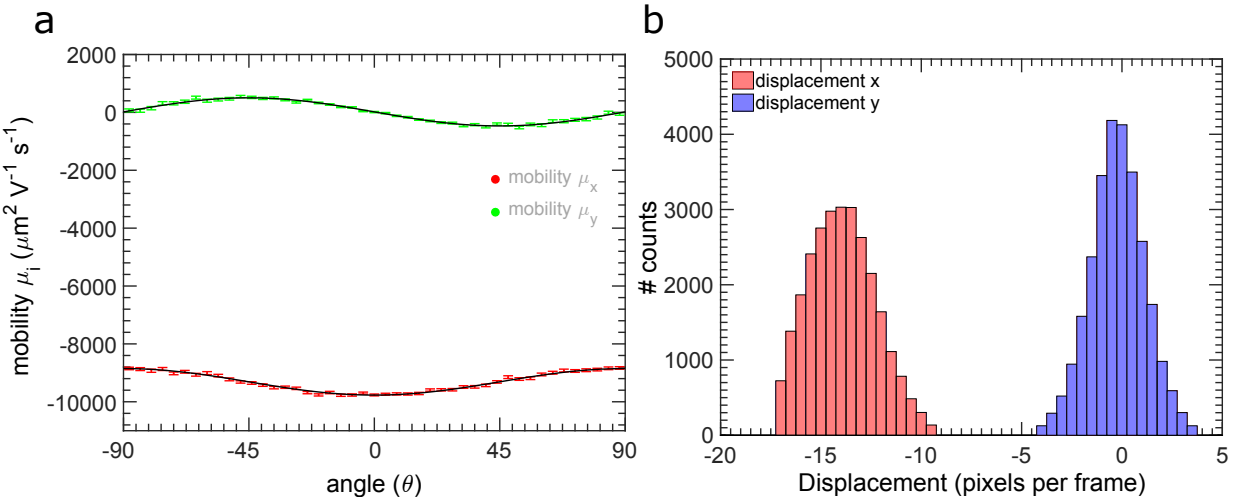

Figure S2: Electrophoresis measurement of R2 silica rods dispersed in DMSO-water, with 0.067 mM LiCl added, $\kappa a = 5.5$. (a) Orientation dependent mobility in x-direction (red symbols), parallel to electric field, and y-direction (green symbols), perpendicular to applied electric field. For clarity raw data is binned in 4° wide bins, the error bars indicate the standard error on the binned data points. The solid lines are a fit through the raw data using equation 10 (μ_x) and equation 11 (μ_y) . (b) Histogram of the displacements of the rods in x and y direction. An anisotropy of $\mu_\perp/\mu_\parallel = 0.906 \pm 0.004$ was found and $\zeta = -70\,mV$, $E = 1.45\,V\,mm^{-1}$, $\Delta t = 0.377\,s$. The error in $\mu_\perp/\mu_\parallel$ is the estimated standard error obtained from the covariance matrix of the fitted parameters.

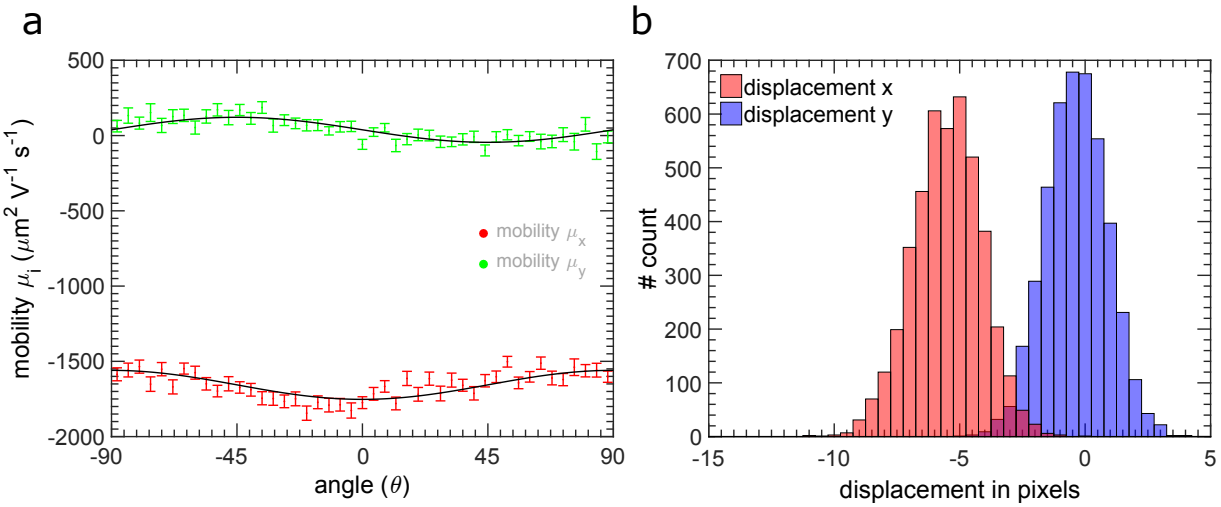

Figure S3: Electrophoresis measurement of SR29 silica rods dispersed in CHC, without salt added, $\kappa a = 0.04$. (a) Orientation dependent mobility in x-direction (red symbols), parallel to electric field, and y-direction (green symbols), perpendicular to applied electric field. For clarity raw data is binned in 4° wide bins, the error bars indicate the standard error on the binned data points. The solid lines are a fit through the raw data using equation 10 (μ_x) and equation 11 (μ_y). (b) Histogram of the displacements of the rods in x and y direction. An anisotropy in mobility of $\mu_\perp / \mu_\parallel = 0.89 \pm 0.02$ was found and $\zeta = -41$ mV, $E = 3.1\,\mathrm{V\,mm^{-1}}$, $\Delta t = 0.374$ s. The error in $\mu_\perp / \mu_\parallel$ is the estimated standard error obtained from the covariance matrix of the fitted parameters.

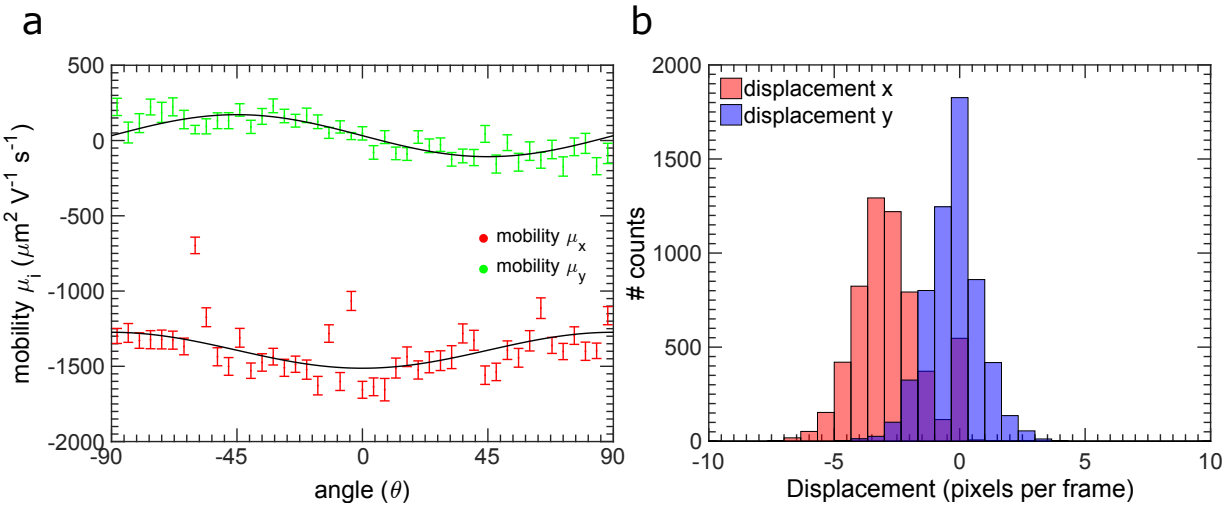

Figure S4: Electrophoresis measurement of SR29 silica rods dispersed in CHC, with TBAC added ($\sim 0.026\,\mu$M), $\kappa a = 0.14$. (a) Orientation dependent mobility in x-direction (red symbols), parallel to electric field, and y-direction (green symbols), perpendicular to applied electric field. For clarity raw data is binned in 4° wide bins, the error bars indicate the standard error on the binned data points. The solid lines are a fit through the raw data using equation 10 (μ_x) and equation 11 (μ_y). (b) Histogram of the displacements of the rods in x and y direction. An anisotropy in mobility of $\mu_\perp / \mu_\parallel = 0.86 \pm 0.05$ was found and $\zeta = -35\,$mV, $E = 3.35\,$V mm^{-1}, $\Delta t = 0.191\,$s. The error in $\mu_\perp / \mu_\parallel$ is the estimated standard error obtained from the covariance matrix of the fitted parameters.

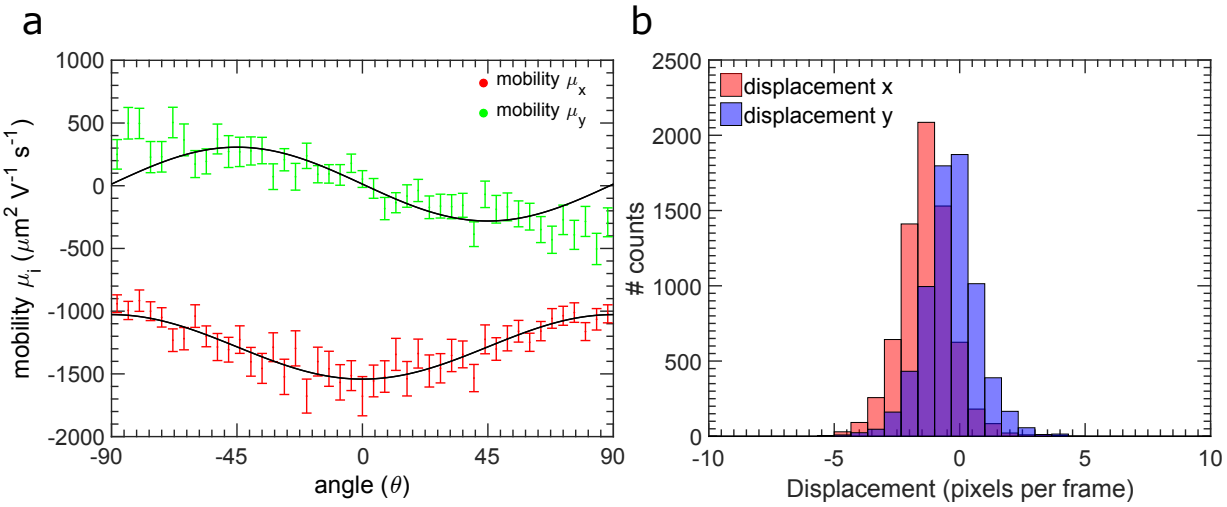

Figure S5: Electrophoresis measurement of SR29 silica rods dispersed in CHC, with TBAC added ($\sim 0.26\,\mu$M), $\kappa a = 0.92$. (a) Orientation dependent mobility in x-direction (red symbols), parallel to electric field, and y-direction (green symbols), perpendicular to applied electric field. For clarity raw data is binned in 4° wide bins, the error bars indicate the standard error on the binned data points. The solid lines are a fit through the raw data using equation 10 (μ_x) and equation 11 (μ_y). (b) Histogram of the displacements of the rods in x and y direction. An anisotropy in mobility of $\mu_\perp / \mu_\parallel = 0.67 \pm 0.03$ was found and $\zeta = -36\,$mV, $E = 3.7\,\mathrm{V\,mm^{-1}}$, $\Delta t = 0.069\,$s. The error in $\mu_\perp / \mu_\parallel$ is the estimated standard error obtained from the covariance matrix of the fitted parameters.

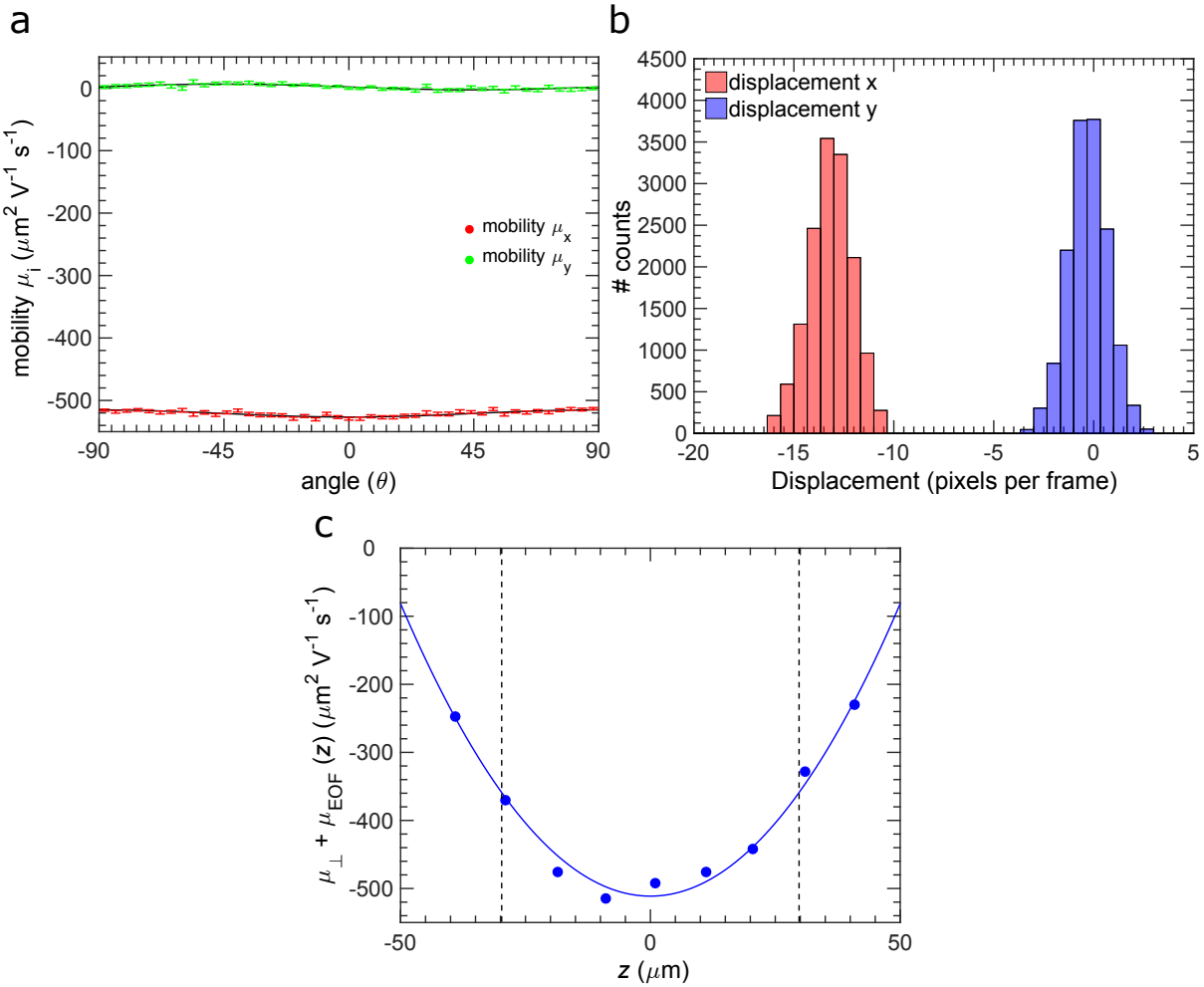

Figure S6: Electrophoresis measurement of R2 silica rods dispersed in 85 wt% glycerol in water, with LiCl added, $\kappa a = 24.5$. (a) Orientation dependent mobility in x-direction (red symbols), parallel to electric field, and y-direction (green symbols), perpendicular to applied electric field. For clarity raw data is binned in 4° wide bins, the error bars indicate the standard error on the binned data points. The solid lines are a fit through the raw data using equation 10 (μ_x) and equation 11 (μ_y). (b) Histogram of the displacements of the rods in x and y direction. (c) Measured electrophoretic mobility profile of rods aligned with the long axis perpendicular to the electric field $\mu_\perp + \mu_{EOF}$ (blue circles), the dashed vertical lines indicate the stationary planes, where we determine μ_{perp}. The center of the capillary is located at $z = 0\,\mu$m. The solid blue line indicate a parabolic-fit through the data. An anisotropy in mobility of $\mu_\perp/\mu_\parallel = 0.98 \pm 0.03$ was found and $\zeta = -68\,$mV, $E = 3.125\,\mathrm{V\,mm^{-1}}$, $\Delta t = 0.863\,$s. The error in $\mu_\perp/\mu_\parallel$ is the estimated standard error obtained from the covariance matrix of the fitted parameters.

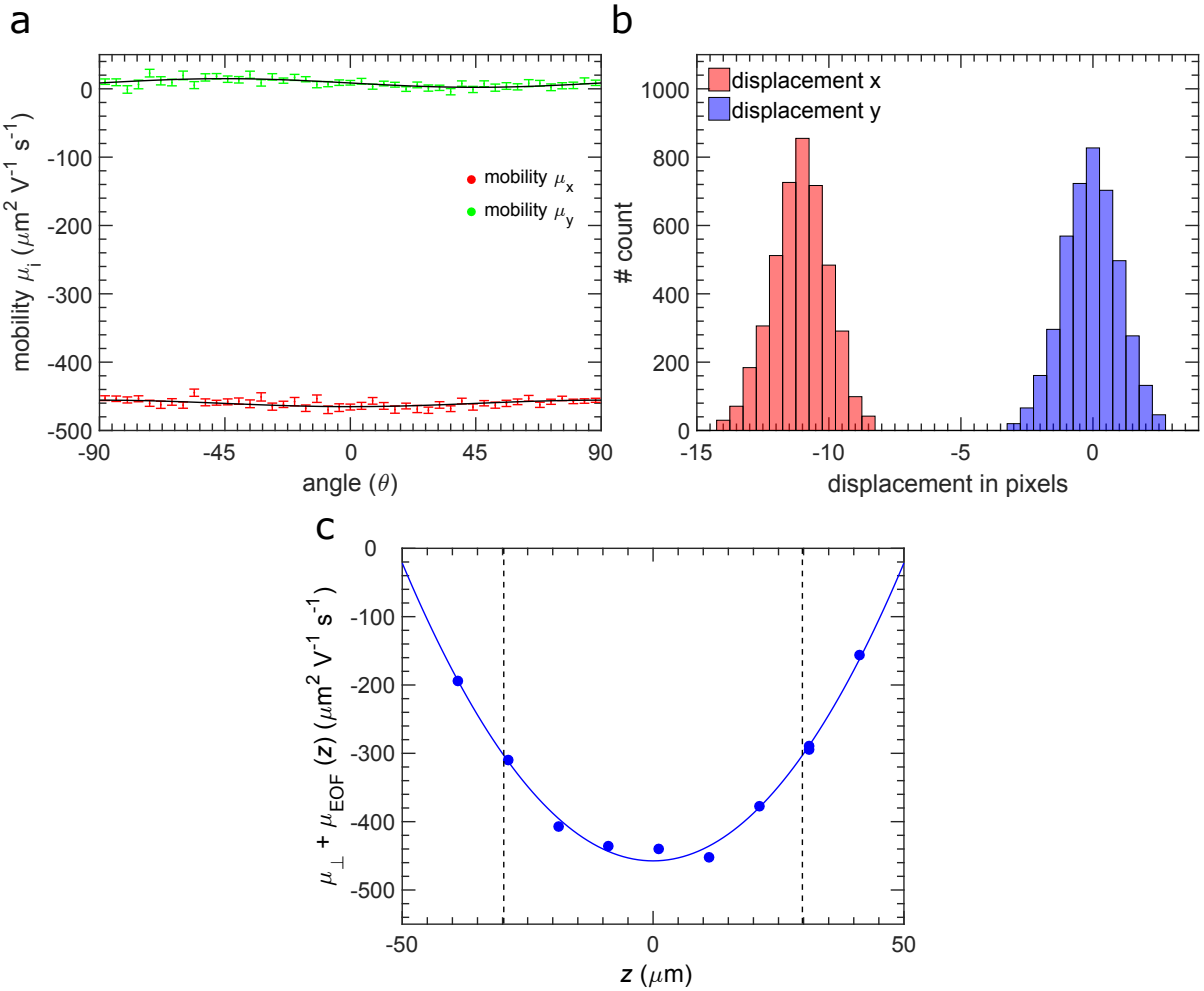

Figure S7: Electrophoresis measurement of R2 silica rods dispersed in 85 wt% glycerol in water, without salt added, $\kappa a = 9.2$. (a) Orientation dependent mobility in x-direction (red symbols), parallel to electric field, and y-direction (green symbols), perpendicular to applied electric field. For clarity raw data is binned in 4° wide bins, the error bars indicate the standard error on the binned data points. The solid lines are a fit through the raw data using equation 10 (μ_x) and equation 11 (μ_y). (b) Histogram of the displacements of the rods in x and y direction. (c) Measured electrophoretic mobility profile of rods aligned with the long axis perpendicular to the electric field $\mu_\perp + \mu_{EOF}$ (blue circles), the dashed vertical lines indicate the stationary planes, where we determine μ_{perp}. The center of the capillary is located at $z = 0\,\mu$m. The solid blue line indicate a parabolic-fit through the data. An anisotropy in mobility of $\mu_\perp/\mu_\parallel = 0.97 \pm 0.02$ was found and $\zeta = -57$ mV, $E = 3\,\mathrm{V\,mm^{-1}}$, $\Delta t = 0.863$ s. The error in $\mu_\perp/\mu_\parallel$ is the estimated standard error obtained from the covariance matrix of the fitted parameters.

Supporting Tables

Table S1: Results on the accuracy of the estimated mobility μ for the particles, three different methods compared. Showing δ, the half-width of the 95% confidence interval for μ, so the 95% confidence interval is $(\mu - \delta, \mu + \delta)$. The bottom section of the table depicts the average δ for the three different methods and the corresponding calculated estimated standard deviation σ. Data on the spheres are taken from Van der Linden *et al.*[1]

R2 rods: Figure 2a measured perpendicular to gravity	**Field strength E** $\mathrm{V\,mm^{-1}}$	**mobility μ** $\mu\mathrm{m^2\,V^{-1}\,s^{-1}}$	**$\pm\,\delta$** $\mu\mathrm{m^2\,V^{-1}\,s^{-1}}$
xyz crosscorrelation	3	−241.0	4.4
xyz crosscorrelation	4	−242.7	2.4
xyt crosscorrelation	3	−245.9	4.4
xyt crosscorrelation	2	−232.6	7.6
xyt particle tracking	3	−253.7	4.7
xyt particle tracking	2	−248.0	19.8

R2 rods: Figure 2b measured parallel to gravity	**Field strength E** $\mathrm{V\,mm^{-1}}$	**mobility μ** $\mu\mathrm{m^2\,V^{-1}\,s^{-1}}$	**$\pm\,\delta$** $\mu\mathrm{m^2\,V^{-1}\,s^{-1}}$
xyz crosscorrelation	3	-242.6	5.7
xyt crosscorrelation	3	-255.4	2.6
xyt particle tracking	3	-271.1	6.9

970 nm silica spheres[1] measured perpendicular to gravity	**Field strength E** $\mathrm{V\,mm^{-1}}$	**mobility μ** $\mu\mathrm{m^2\,V^{-1}\,s^{-1}}$	**$\pm\,\delta$** $\mu\mathrm{m^2\,V^{-1}\,s^{-1}}$
xyz crosscorrelation	3	−291.6	1.9
xyt crosscorrelation	3	−288.8	39.6
xyt particle tracking	3	−288.8	39.2

970 nm silica spheres[1] measured parallel to gravity	**Field strength E** $\mathrm{V\,mm^{-1}}$	**mobility μ** $\mu\mathrm{m^2\,V^{-1}\,s^{-1}}$	**$\pm\,\delta$** $\mu\mathrm{m^2\,V^{-1}\,s^{-1}}$
xyz crosscorrelation	3	−293.0	3.7
xyt crosscorrelation	3	−289.0	5.9
xyt particle tracking	3	−284.2	11.0

930 nm silica spheres[1] measured perpendicular gravity	**Field strength E** $\mathrm{V\,mm^{-1}}$	**mobility μ** $\mu\mathrm{m^2\,V^{-1}\,s^{-1}}$	**$\pm\,\delta$** $\mu\mathrm{m^2\,V^{-1}\,s^{-1}}$
xyz crosscorrelation	3	−213.8	2.0
xyz crosscorrelation	5	−209.0	1.1
xyt crosscorrelation	3	−205.4	7.1
xyt particle tracking	3	−205.8	8.1

Measurement method	**average δ** $\mu\mathrm{m^2\,V^{-1}\,s^{-1}}$	**σ** $\mu\mathrm{m^2\,V^{-1}\,s^{-1}}$
xyz crosscorrelation	3.0	0.8
xyt crosscorrelation	11.2	4.9
xyt particle tracking	14.9	4.6

References

(1) van der Linden, M. N.; Helfferich, K. M., P. H.; Wijnhoven, J. E. G. J.; Bakker, H. E.; van Blaaderen, A. in preparation.